

PAPR REDUCTION IN CP-OFDM (5G) USING HYBRID TECHNIQUE

AZLAN YUSOF, AZLINA IDRIS*, EZMIN ABDULLAH

Universiti Teknologi MARA, School of Electrical Engineering, Wireless Communication Technology Group (WICOT), 40450 Shah Alam Selangor, Malaysia

* corresponding author: azlina831@uitm.edu.my

ABSTRACT. The Cyclic Prefix Orthogonal Frequency Division Multiplexing (CP-OFDM) is a 5G multi-carrier waveform that offers great data speeds and improvements in spectrum utilisation. The primary CP-OFDM's weakness is its excessive peak-to-average power ratio (PAPR), which is a characteristic of all multicarrier modulation techniques. We study the application of a hybrid technique approach how to lower the peak to average power ratio (PAPR) in a CP-OFDM system. We also evaluated the outcomes of peak to average power ratio (PAPR) decrease in CP-OFDM, utilising a hybrid technique with Group Codeword Shift (GCS), Median Codeword Shift, Selective Codeword Shift (SCS), and Conventional CP-OFDM. When compared to the non-hybrid technique, the simulation results indicate that the hybrid approach is superior in reducing the peak PAPR by more than 65 percent.

KEYWORDS: Cyclic prefix orthogonal frequency division multiplexing (CP-OFDM), peak to average power ratio (PAPR), hybrid technique, group codeword shift (GCS).

1. INTRODUCTION

Much research and study has been done on how to overcome a high PAPR value by introducing ways for lowering the PAPR value, which can be classified into three main approaches [1, 2]. The first one, signal scrambling techniques, can be divided into the following categories: Selective Mapping (SLM), Partial Transmit Sequence (PTS), Selective Codeword Shift (SCS), Median Codeword Shift (MCS), Interleaving, Tone Reservation (TR), Tone Injection (TI), and Active Constellation Extension (ACE). The second one, Signal Distortion Techniques, can be divided into the following classifications: Clipping and Filtering, Compounding, Peak Windowing, and Envelope Scaling. And the third one, signal coding techniques, can be divided into: block coding and turbo coding [1, 2]. While previous research has demonstrated the potential for PAPR minimisation, it has also encountered trade-offs, such as increased computational complexity, side information, loss of data rate and bandwidth, loss of spectral efficiency, and distortion. The Block Coding approach can be divided into two types: Arithmetic coding and Huffman coding; Arithmetic coding is more effective in reducing PAPR than Huffman coding. Clipping and filtering is the simplest strategy to reduce PAPR and it is dependent on the clipping intensity that satisfies the signal to quantisation noise ratio (SQNR) [3].

In comparison to SLM and clipping and filtering techniques, the PTS approach is more effective in reducing PAPR values [4]. The Selected Mapping (SLM) approach involves applying numerous phase rotations to the constellation points and selecting the one that minimises the time signal peak. The selected mapping also involves generating a large number of

vectors with the lowest resulting PAPR. The transmit signal with the lowest PAPR is selected from a group of suitably distinct signals that all reflect the same data. The advantage of SLM is that no distortion is introduced and the number of carriers is independent, while the disadvantage is that side information is introduced and the BER performance is degraded [5–7]. Because of this drawback, PAPR has been reduced using a mix of SLM and clipping techniques [8]. SLM can be enhanced with M-QAM technology to increase the PAPR value by approximately 3.4 dB [4]. While the SLM approach decreases the PAPR value, it also reduces the system's data rate and computing complexity. To determine which technique is capable of reducing a high PAPR value, several criteria must be considered, including the data rate loss and computational complexity at the receiver, power increase in the transmitted signal, PAPR reduction capability, and bandwidth expansion [9, 10]. Although the Selective Codeword Shift (SCS) approach has shown a significant improvement in PAPR reduction compared to the original signal and conventional SLM, this technique is only applicable to modulations greater than 4 QAM or 2 bits per symbol. The benefit of this approach is that it has a lower computational cost than the SLM due to the usage of IFFT blocks and the absence of phase factor multiplication during the transmission process [11, 12]. The codeword in the SCS approach is a circulant shift, and the time required to complete this circulant shift is greater due to the codeword's extended course of travel. As a result, the PAPR and BER values are not significantly reduced with the SCS approach. The Group Codeword Shifting (GCS) technique is proposed in this study; the codeword is divided into two parts (part A and

part B) to facilitate codeword shifting. PAPR has a lower GCS value than SCS and MCS methods. The Companding method was chosen to be combined with the GCS, SCS and MCS methods because it reduces the system complexity and significantly reduces the PAPR. To the best of our knowledge, no research on combining the companding method with GCS, SCS, and MCS methods in order to reduce PAPR has yet to be carried out.

2. METHODOLOGY

2.1. CP-OFDM

Since January 2016, the 3rd Generation Partnership Project (3GPP) has been developing to standardise 5G New Radio (NR), a new Radio Access Technology (RAT) that will assure the reliability, synergy, and excellence of next-generation 5G devices and networks. This enables the development of cyber experience, immersive reality, artificial intelligence, self-driving cars, and the Internet of Things (IoT). To provide these services, a next generation of wireless telecommunication technologies will be required, and consequently, systems will need a reliable, rapid, and even quicker connections [13]. In order to enable all of the operations that the 5G standard is designed to deliver, 5G NR must address three key issues: higher data speeds, transmissions with higher durability and lower latency, and a significant increase in the number of devices. The motivations leading to the three main use cases include [14]: enhanced mobile broadband (eMBB) which requires massive transmission speeds and huge bandwidths [14]. Second, ultra-reliable low-latency communications (uRLLC), which requires extremely high reliability and availability in addition to very low latency [15]. Finally, massive machine-type communications (mMTC) which requires extremely low power consumption [16].

The 3GPP selected CP-OFDM for both the downlink and the uplink physical-layer radio access in the NR Release 15 [17]. Because the 5G NR is based on OFDM (as is LTE), it benefits from the fact that it allows equipment to maintain a low level of functionality and therefore low hardware costs. In addition, a single OFDM numerology defined by subcarrier spacing and cyclic prefix length is unable to achieve capacity limits throughout the required frequency spectrum and entire recommended placement choices and scenarios. Therefore, the OFDM numerology must be customised for each service demand, operating frequency, and deployment environment [14, 18]. The cyclic prefix (CP) orthogonal frequency-division multiplexing (OFDM) was chosen for its various advantages, including good support for multiple-input multiple-output (MIMO) and granularity in frequency-domain resource allocation [17]. OFDM's notable drawbacks include a high out-of-band (OOB) power consumption [19], frequency offset susceptibility [19], and high peak-to-average power ratio (PAPR) [20]. The large

peak-to-average power ratio (PAPR) of any multi-carrier system, including CP-OFDM, is a significant disadvantage. This is caused by the time domain random insertion of subcarriers. Consider the four sinusoidal impulses below, each with a different frequency and phase shift. When the peak amplitudes of a number of signals coincide, the resulting signal envelope shows prominent peaks. According to the transmitter's large peaks, the power amplifier operates in the nonlinear zone, causing a deformation and spectrum propagation. Furthermore, as the number of subcarriers grows, so does the fluctuation of the output power [21]. Apart from CP-OFDM, the out-of-band (OOB) emission is extremely efficient in the time domain, necessitating time, and frequency synchronisations due to interference with neighbouring channels caused by the OOB emission. Because the constrained synchronisation adds additional time (latency) to the functioning of the system, this increased latency requires increased power usage [22].

Cyclic Prefix (CP) is a copy of the Orthogonal Frequency-Division Multiplexing (OFDM) symbol waveform tail that is injected at the start to decrease the multipath channel lag dispersion and the consequent intersymbol interference (ISI). As a consequence, with a proper temporal sampling of the received signal and a CP length much greater than the highest expected channel lag dispersion, not only ISI but also Intercarrier Interference (ICI) is eliminated [23, 24]. The CP's length is dictated by the impulse reaction of the transmission channel. In a communication network, the selection of CP is controlled by the propagation conditions and cell size. Despite its multipath resistant channels, implementing CP-OFDM in wireless transmitters faces several obstacles. The CP-OFDM signals employ CP over a length of time greater than the temporal channel's extent, resulting in a loss in spectral efficiency [25, 26]. CP-OFDM begins with baseband modulation of the source symbols using one of the modulation standards such as QAM. The IFFT method then transforms the modulated symbols X_k from the frequency domain (FD) to the time domain (TD), resulting in the discrete baseband OFDM signal $x(n)$ [27].

$$x(n) = \frac{1}{\sqrt{N}} \sum_{K=0}^{N-1} X_k e^{j2\pi k \frac{n}{N}}, \quad (1)$$

where $n = 0, 1, 2, \dots, N - 1$, where N denotes the subcarrier count. The discrete baseband OFDM signal is formed by orthogonally superimposing the input data symbol's K -samples on top of the N -subcarriers. In OFDM, by inserting the last component of the OFDM signal in front of the OFDM symbol, the signal is protected against inter-symbol interference (ISI). However, the OFDM signal is formed by combining N -modulated subcarriers. As a result, when the samples have comparable phases, the power of selected samples may surpass the signal's average power.

Therefore, the PAPR value can be stated as the ratio of the maximum continuous power of the signal to its mean power divided by the maximum instantaneous power of the signal [27].

$$PAPR = \frac{|max(n)|^2}{E|x(n)|^2}, \quad (2)$$

where E is the mean value. Additionally, the complementary cumulative distribution function (CCDF) is widely used to estimate the probability of PAPR value surpassing a predefined threshold value [27].

$$Pr(PAPR > PAPR_0) = 1 - (1 - exp(-PAPR_0))^{NL}, \quad (3)$$

where $PAPR_0$ denotes the threshold value and L denotes the oversampling factor used to convert the characteristics of the discrete-time signal to those of a continuous-time signal; this is accomplished by embedding $(L - 1)N$ zeros in the FD samples [27–29].

2.2. CP-OFDM BASED ON HYBRID TECHNIQUE

Merging two or several techniques will result in a hybrid technique that provides a significant improvement in PAPR, but also inherits the limitations of the original techniques. The SLM procedure minimises the PAPR value while simultaneously compromising the system’s data throughput and computing complexity. For selecting which technique can reduce a high PAPR value, few criteria need to be taken into account, such as data rate loss, computational complexity, power increment in the transmitted signal, PAPR reduction capability, and bandwidth expansion [30]. The Companding technique is usually used in the hybrid technique due to its simplicity compared to other techniques. In this research, the hybrid technique combines the Group Codeword Shift method with the Companding A-law and Mu-law methods to reduce the value of PAPR. By using non-uniform quantisation characteristics, a high-amplitude PAPR signal is compressed and a low-amplitude output is boosted to maintain the mean power during the companding conversion [31–33]. This Companding technique has already proven its efficiency for PAPR problems with less implementation complexity. The principle of compression technology is twofold: the signal’s amplitude is compressed at the transmitter before being expanded once more at the receiver. The following function can be used to compress a CP-OFDM signal using Mu-law [34].

$$G(x) = \text{sgn}(x) \frac{\ln(1 + \mu|x|)}{\ln(1 + \mu)}, \quad (4)$$

$$G^{-1}(x) = \frac{|x|(1 + \ln(A))}{A}, |x| < \frac{1}{1 + \ln(A)}, \quad (5)$$

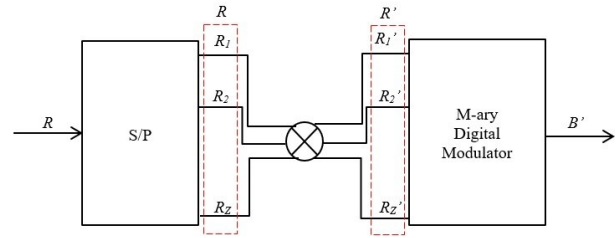


FIGURE 1. GCS sub-block.

$$G^{-1}(x) = \frac{exp(|x|(1 + \ln(A)) - 1)}{A}, \frac{1}{1 + \ln(A)} < |x| < 1, \quad (6)$$

where the A indicates the compression parameter, which is usually set at 87.6 [35]. The expansion function for A-law can be expressed as above [34].

Another technique that can be combined with Companding to form a hybrid is Group Codeword Shifting. By changing the codeword format and then utilising a recombination process (circulant shift) to create a scrambled input series, the shifting approach creates a new codeword that is better at reducing PAPR. This Group Codeword Shifting technique is aiming at the arrangement of the codeword and the structure of the bits in reducing PAPR. By manipulating these two parameters, an alternative codeword with a lower PAPR is generated. R stands for the binary series codeword with r total input bits, as illustrated in Figure 1, and can be written as $R = [R_1, R_2, \dots, R_r]$. The series-to-parallel conversion splits the codeword series into z sub blocks denoted by $R = [R_1, R_2, \dots, R_z]$ and each sub-block contains y number of bits per symbol, where $z = r/y$. As a result, the codeword description for each different sub block can be expressed as $R_1 = [R_{1,1}, R_{1,2}, R_{1,3}, \dots, R_{1,y}]$, $R_2 = [R_{2,1}, R_{2,2}, R_{2,3}, \dots, R_{2,y}]$, up to R_z .

The first step performed by the group codeword shifting technique is to modify the arrangement by splitting the codeword into parts A and B as shown in Figure 3. The alternate codeword is generated in the second stage by applying the circulant shift between parts A and B once per period. Table 1 shows the position of the bits during the modification operations for clarity. Codeword $R_{1,0}$ indicates the starting location of the bits of the codeword. As a result of the switching between part A and part B, the modified bit position is indicated by the codeword $R_{1,1}$. The proposed alternate series of codewords are written as $R' = [R'_1, R'_2, \dots, R'_z]$. Finally, the CP-OFDM signal with the lowest PAPR value is selected for transmission.

Figure 2 shows the first phase of the group codeword shifting approach, which involves modifying the layout of the codeword by splitting it into two components, A and B. A new codeword is generated in the second

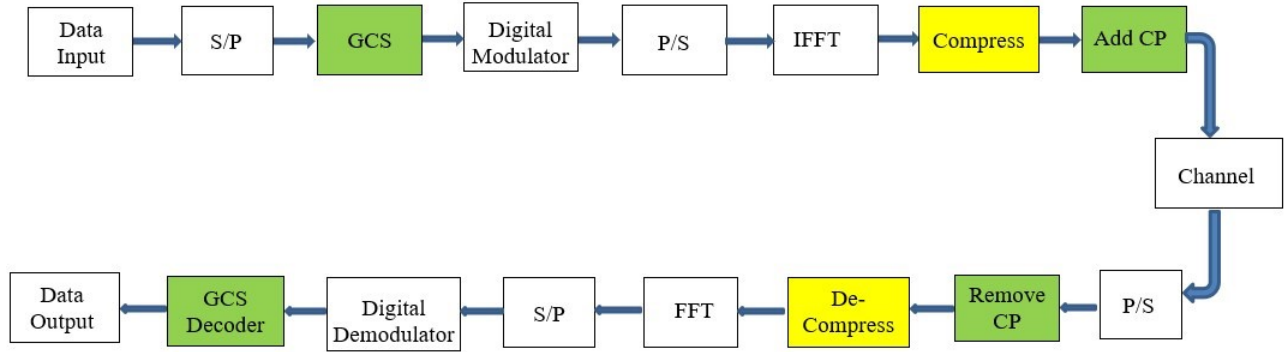


FIGURE 2. Block diagram of hybrid technique.

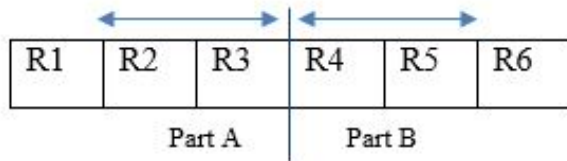


FIGURE 3. Group Codeword Shifting structure.

Sub-block codeword bits, $R_{z,\delta}$	Structure of bits
Codeword, $R_{1,0}$	$R_1, R_2, R_3, R_4, R_5, R_6$
Codeword shift 1, $R_{1,1}$	$R_4, R_2, R_3, R_1, R_5, R_6$
Codeword shift 2, $R_{1,2}$	$R_1, R_4, R_3, R_2, R_5, R_6$
Codeword shift 3, $R_{1,3}$	$R_1, R_2, R_4, R_3, R_5, R_6$
Codeword shift 4, $R_{1,4}$	$R_5, R_2, R_3, R_4, R_1, R_6$
Codeword shift 5, $R_{1,5}$	$R_1, R_5, R_3, R_4, R_2, R_6$
Codeword shift 6, $R_{1,6}$	$R_1, R_2, R_5, R_4, R_3, R_6$
Codeword shift 7, $R_{1,7}$	$R_6, R_2, R_3, R_4, R_5, R_1$
Codeword shift 8, $R_{1,8}$	$R_1, R_6, R_3, R_4, R_5, R_2$
Codeword shift 9, $R_{1,9}$	$R_1, R_2, R_6, R_4, R_5, R_3$

* Proposed compression technique

TABLE 1. The bit configuration for Group Codeword Shifting technique.

stage by applying the circulant random shift between the Component A and B individually. Component A consists of R_1, R_2 and R_3 while Component B consists of R_4, R_5 and R_6 . The R_1 of Component A and R_4 of Component B are shifted first. In the second shifting, R_1 returns to its original position in Component A, R_2 replaces the R_1 position of Component B, and R_4 fills the R_2 original position in Component A. In the third shifting process, R_2 returns to its original position in Component A, R_3 replaces the R_2 position of Component B, and R_4 fills R_3 original position in Component A. For more details about the shifting process, see the illustration in Table 1 for the location of the bits after the shifting operations. The Codeword $R_{1,0}$ represents the beginning location of the codeword's bits. As a result of the shifting between part A and part B, the modified bit state will be denoted as Codeword

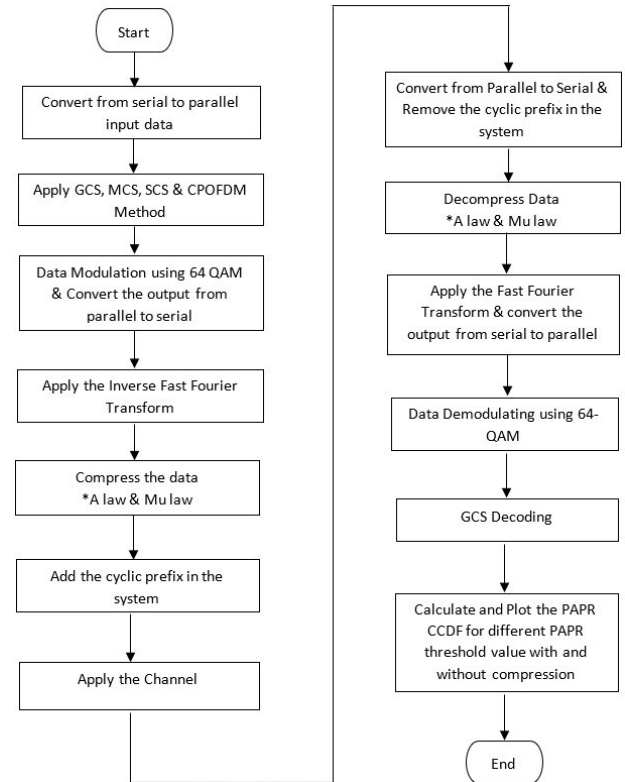


FIGURE 4. Simulation flowchart.

$R_{1,1}$. The revised alternate series of codewords are written as $R' = [R'_1, R'_2, \dots, R'_z]$. Therefore, the CP-OFDM signal option with the lowest PAPR value can be selected for propagation. The entire simulation process is depicted in Figure 4.

3. RESULTS AND DISCUSSION

A simulation was developed in MATLAB software and around 15,000 iterations were used to analyse the reliability of the PAPR. $N = 128$ random incoming subcarriers were generated and mapped in the simulation utilising 64-QAM modulation. The CP-OFDM signal was sent to the AWGN channel. The cyclic prefix having a period of $1/4$ was introduced to the CP-OFDM symbols to reduce the inter-symbol interference (ISI). Table 2 provides a comprehensive list of

Parameter	Value
Bandwidth (BW)	8068.58 Hz
FFT length	512
Tone offset	2.5
L (filter length)	512
Modulation Technique	64QAM
Cyclic Prefix Length	1/4
Channel Model	AWGN

TABLE 2. Modelling variables [27].

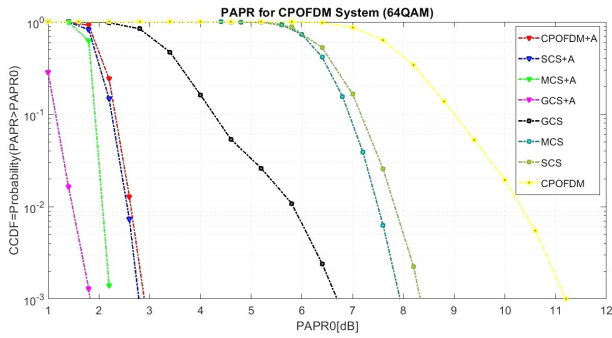


FIGURE 5. PAPR effectiveness evaluation for hybrid A law technique with GCS, MCS, SCS, and CP-OFDM.

all simulation-related variables.

Figure 5 shows the PAPR performance for the hybrid A Law technique combination with SCS, MCS, GCS, and CP-OFDM, compared to the original SCS, MCS, GCS and CP-OFDM. A summary of the graph at CCDF 10^{-3} in Table 3 shows that the original value of CP-OFDM is 11.2 dB, while for the hybrid A law of CP-OFDM, it is 2.90 dB at CCDF Probability 10^{-3} , which is 74.11 % improvement for the hybrid A law technique over the original value of CP-OFDM. The hybrid A law combination with SCS and MCS techniques provides an improvement of 66.51 % and 71.9 % over the original SCS and MCS techniques, respectively. Furthermore, the hybrid A law combination with the GCS technique provides the highest improvement of 72.84 %, as compared with the hybrid A law combination with SCS and MCS techniques and also the lowest PAPR value of 1.82 dB. The result is influenced by the random arrangement of the several lowest PAPR possibilities. The GCS technique is able to provide multiple candidates, so more choices can be used. However, shifting too far will not affect the PAPR result. Another factor is the random order of the bits. The greater the number of candidates, the greater the number of random order of the shifts will be generated. And consequently, the greater the number of random order of the shifts, the better the PAPR value [35].

Figure 6 shows the PAPR performance for the hybrid Mu Law Technique combination with SCS, MCS, GCS, and CP-OFDM compared to the original SCS, MCS, GCS and CP-OFDM. A summary of the graph

Parameter	PAPR	% Of Improvement
CP-OFDM	11.2	–
CP-OFDM A LAW	2.90	74.11
SCS	8.30	–
SCS A LAW	2.78	66.51
MCS	7.90	–
MCS A LAW	2.22	71.90
GCS	6.70	–
GCS A LAW	1.82	72.84

TABLE 3. PAPR analysis with hybrid A law technique and non-hybrid techniques.

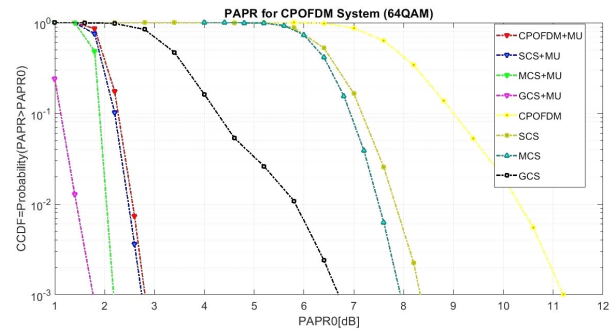


FIGURE 6. PAPR performance for hybrid Mu law with GCS, MCS, SCS, and CP-OFDM.

at CCDF 10^{-3} in Table 3 shows that the original value of CP-OFDM is 11.2 dB, while for the hybrid Mu law of CP-OFDM, it is 2.81 dB at CCDF Probability 10^{-3} , which is 74.19 % improvement for the hybrid Mu law technique over the original value of CP-OFDM. The hybrid Mu law combination with SCS and MCS techniques provides an improvement of 67.23 % and 72.41 % over the original SCS and MCS techniques, respectively. Furthermore, the hybrid Mu law combination with GCS technique provides the highest improvement of 73.43 % as compared to the hybrid Mu law combination with SCS and MCS and also the lowest PAPR value of 1.78 dB. The result is influenced by the random arrangement of the several lowest PAPR possibilities. The GCS technique is able to provide multiple candidates, so more choices can be used. However, shifting too far will not affect the PAPR result. Another factor is the random order of the bits. The greater the number of candidates, the greater the number of random order of the shifts will be generated. And consequently, the greater the number of random order of the shifts, the better the PAPR value [35].

4. CONCLUSION

This article describes a hybrid precoding technique, a simple technique with low complexity that is recommended to reduce PAPR, which is the main problem of CP-OFDM systems [36, 37]. The hybrid technique has shown a significant improvement in reducing high

Parameter	PAPR	% Of Improvement
CP-OFDM	11.2	–
CP-OFDM A LAW	2.81	74.91
SCS	8.30	–
SCS A LAW	2.72	67.23
MCS	7.90	–
MCS A LAW	2.18	72.41
GCS	6.70	–
GCS A LAW	1.78	73.43

TABLE 4. PAPR analysis of hybrid Mu law technique and non-hybrid techniques.

PAPR as compared to MCS, SCS, GCS, and the original CP-OFDM signal. The combination of the GCS method with Companding A and Mu law for the hybrid technique has been proposed because of its potential to reduce PAPR in CP-OFDM systems. The GCS has shown a significant improvement in reducing high PAPR as compared to MCS, SCS, and the original CP-OFDM signal in the hybrid technique. Furthermore, the hybrid A law of the GCS gives the highest improvement of 72.84% compared to the hybrid A law, SCS, and MCS and also the lowest PAPR value of 1.82 dB. The hybrid Mu law of GCS gives the highest improvement of 73.43% compared to the hybrid Mu law, SCS, and MCS and also the lowest PAPR value of 1.78 dB.

The Group Codeword Shifting (GCS) technique generates the alternative codeword by altering the structure of the codeword followed by a permutation process (circulant shift) in order to generate a scrambled data sequence for better PAPR reduction. This Group Codeword Shifting technique aims for the arrangement of the codeword and the bit structure that reduce PAPR, by manipulating these two parameters, the alternative codeword with lower PAPR is created. For this reason, the GCS hybrid technique is better than MCS hybrid and SCS hybrid at reducing PAPR. However, this method has a limitation, it is only effective for modulations higher than 4 QAM, because the shift algorithm need more than 2 bits to perform the shifting process. The advantage of the GCS hybrid method is a low computational complexity, achieved by reducing the use of IFFT block in the system, as compared to MCS hybrid, SCS hybrid and the original CP-OFDM. The hybrid technique is applied at the transceiver. Further research is recommended to investigate the efficiency of reducing the PAPR in different modulation approaches for other applications.

REFERENCES

- [1] J. Umarji, A. S. Awati, S. P. Deshpande. PAPR reduction technique in OFDM. *International Journal of Scientific Research in Science, Engineering and Technology* **2**(3):757–760, 2016.
- [2] M. Bisht, A. Joshi. Various techniques to reduce PAPR in OFDM systems: A survey. *International Journal of Signal Processing, Image Processing and Pattern Recognition* **8**(11):195–206, 2015. <https://doi.org/10.14257/ijpsip.2015.8.11.18>
- [3] O. S. Al-Heety, M. Ismail, Z. Zakaria, M. A. Altahrawi. Performance evaluation of peak-to-average-power ratio reduction techniques in OFDM. *International Journal of Engineering Research and Technology* **11**(4):575–593, 2018.
- [4] M. Selvakumer, B. Sudhakar. Peak to average power ratio reduction for filtered OFDM modulation in 5G frameworks using hybrid techniques. *Annals of the Romanian Society for Cell Biology* **25**(1):4302–4320, 2021.
- [5] M. M. Rahman, M. N. A. S. Bhuiyan, M. S. Rahim, S. Ahmed. A computationally efficient selected mapping technique for reducing PAPR of OFDM. *Telecommunication Systems* **65**:637–647, 2017. <https://doi.org/10.1007/s11235-016-0257-0>
- [6] E. Abdullah, A. Idris, A. Saparon. Modified selective mapping scheme with low complexity for minimizing high peak-average power ratio in orthogonal frequency division multiplexing system. In *Proceedings of the 1st International Conference on Advanced Science, Engineering and Technology*, vol. 1774, p. 050005. 2016. <https://doi.org/10.1063/1.4965092>
- [7] E. Abdullah, A. Idris, A. Saparon. Performance evaluation of modified SLM technique in OFDM system using selected codeword shift. In *MATEC Web of Conferences*, vol. 75, p. 06003. 2016. <https://doi.org/10.1051/mateconf/20167506003>
- [8] R. A. Malik, R. Singla. To study the different techniques to reduce the PAPR in OFDM system. *International Journal of Electrical Engineering* **9**(1):67–75, 2016.
- [9] S. Prasad, R. Jayabalan. PAPR reduction in OFDM systems using modified SLM with different phase sequences. *Wireless Personal Communications* **110**:913–929, 2020. <https://doi.org/10.1007/s11277-019-06763-7>
- [10] M. Fallahzadeh, M. Ferdosizadeh. Blind SLM for PAPR reduction of Alamouti DSFBC systems. *IET Communications* **11**(3):451–457, 2017. <https://doi.org/10.1049/iet-com.2016.0340>
- [11] E. Abdullah, A. Idris. Selective codeword shift (SCS) technique for PAPR reduction of OFDM systems. *Jurnal Teknologi* **78**(5–9):59–65, 2016. <https://doi.org/10.11113/jt.v78.8788>
- [12] E. Abdullah, A. Idris, A. Saparon. Minimizing high PAPR in OFDM system using circulant shift codeword. *Jurnal Teknologi* **78**(2):135–140, 2016. <https://doi.org/10.11113/jt.v78.4890>
- [13] R. Ravindran, A. Viswakumar. Performance evaluation of 5G waveforms: UFMC and FBMC-OQAM with cyclic prefix-OFDM system. In *9th International Conference on Advances in Computing and Communication (ICACC)*, pp. 6–10. 2019. <https://doi.org/10.1109/ICACC48162.2019.8986195>

- [14] J. F. de Vargas, J. F. Monserrat, H. Arslan. Flexible numerology in 5G NR: Interference quantification and proper selection depending on the scenario. *Mobile Information Systems* **2021**:6651326, 2021. <https://doi.org/10.1155/2021/6651326>
- [15] R. Ayadi, I. Kammon, M. Siala. Bridging the gap between CP-OFDM and ZP-OFDM for the provision of ultra-low latency services in 5G. *IEEE Systems Journal* **14**(1):603–613, 2020. <https://doi.org/10.1109/JSYST.2019.2924249>
- [16] C. Bockelmann, N. Pratas, H. Nikopour, et al. Massive machine-type communications in 5G: Physical and MAC-layer solutions. *IEEE Communications Magazine* **54**(9):59–65, 2016. <https://doi.org/10.1109/MCOM.2016.7565189>
- [17] S. Gökceli, T. Levanen, T. Riihonen, et al. Novel iterative clipping and error filtering methods for efficient papr reduction in 5G and beyond. *IEEE Open Journal of the Communications Society* **2**:48–66, 2021. <https://doi.org/10.1109/OJCOMS.2020.3043598>
- [18] J. Yli-Kaakinen, T. Levanen, S. Valkonen, et al. Efficient fast-convolution-based waveform processing for 5G physical layer. *IEEE Journal on Selected Areas in Communications* **35**(6):1309–1326, 2017. <https://doi.org/10.1109/JSAC.2017.2687358>
- [19] G. Kongara, C. He, L. Yang, J. Armstrong. A comparison of CP-OFDM, PCC-OFDM and UFMC for 5G uplink communications. *IEEE Access* **7**:157574–157594, 2019. <https://doi.org/10.1109/ACCESS.2019.2949792>
- [20] K. Tahkoubit, A. Ali-Pacha, H. Shaiek, D. Roviras. PAPR reduction of BF-OFDM waveform using DFT-spread technique. In *16th International Symposium on Wireless Communication Systems (ISWCS)*, pp. 406–410. 2019. <https://doi.org/10.1109/ISWCS.2019.8877195>
- [21] A. F. Demir, M. Elkourdi, M. Ibrahim, H. Arslan. Waveform design for 5G and beyond. In *5G Networks: Fundamental Requirements, Enabling Technologies, and Operations Management*. 2018. Chap. 2. <https://doi.org/10.1002/9781119333142.ch2>
- [22] A. A. Sahrab, A. D. Yaseen. Filtered orthogonal frequency division multiplexing for improved 5G systems. *Bulletin of Electrical Engineering and Informatics* **10**(4):2079–2087, 2021. <https://doi.org/10.11591/eei.v10i4.3119>
- [23] A. Lipovac, V. Lipovac, B. Modlic. PHY, MAC, and RLC layer based estimation of optimal cyclic prefix length. *Sensors* **21**(14):4796, 2021. <https://doi.org/10.3390/s21144796>
- [24] M. Bozic, D. Barjamovic, M. Cabarkapa, D. Budimir. Waveform comparison and PA nonlinearity effects on CP-OFDM and 5G FBMC wireless systems. *Microwave and Optical Technology Letters* **60**(8):1952–1956, 2018. <https://doi.org/10.1002/mop.31272>
- [25] A. Hammoodi, L. Audah, M. A. Taher. Green coexistence for 5G waveform candidates: A review. *IEEE Access* **7**:10103–10126, 2019. <https://doi.org/10.1109/ACCESS.2019.2891312>
- [26] F. M. Mustafa, H. M. Bierk, M. N. Hussain. Reduction of PAPR pattern with low complexity using hybrid-PTS scheme for the 4G and 5G multicarrier systems. *Journal of Engineering Science and Technology* **16**(4):3481–3504, 2021.
- [27] H. Shaiek, R. Zayani, Y. Medjahdi, D. Roviras. Analytical analysis of SER for beyond 5G post-OFDM waveforms in presence of high power amplifiers. *IEEE Access* **7**:29441–29452, 2019. <https://doi.org/10.1109/ACCESS.2019.2900977>
- [28] J. Park, E. Lee, S.-H. Park, et al. Modeling and analysis on radio interference of OFDM waveforms for coexistence study. *IEEE Access* **7**:35132–35147, 2019. <https://doi.org/10.1109/ACCESS.2019.2896280>
- [29] S. Kaur, G. Saini. Review paper on PAPR reduction techniques in OFDM system. *Indian Journal of Science and Technology* **9**(48):1–6, 2017. <https://doi.org/10.17485/ijst/2016/v9i48/106893>
- [30] R. D. Kanti, R. V. C. S. Rao. Systematic comparison of different PAPR reduction methods in OFDM systems. *International Journal of Electronics and Communication Engineering* **7**(1):21–30, 2014.
- [31] M. I. Al-Rayif, H. Seleem, A. Ragheb, S. Alshebeili. A novel iterative-SLM algorithm for PAPR reduction in 5G mobile fronthaul architecture. *IEEE Photonics Journal* **11**(1):1–12, 2019. <https://doi.org/10.1109/JPHOT.2019.2894986>
- [32] A. Kumar, M. Gupta. A review on OFDM and PAPR reduction techniques. *American Journal of Engineering and Applied Sciences* **8**(2):202–209, 2015. <https://doi.org/10.3844/ajeassp.2015.202.209>
- [33] M. H. Aghdam, A. A. Sharifi. PAPR reduction in OFDM systems: An efficient PTS approach based on particle swarm optimization. *ICT Express* **5**(3):178–181, 2019. <https://doi.org/10.1016/j.icte.2018.10.003>
- [34] M. Selvakumar, B. Sudhakar. Peak to average power ratio reduction for filtered OFDM modulation in 5G frameworks using hybrid techniques. *Annals of the Romanian Society for Cell Biology* **25**(1):4302–4320, 2021.
- [35] A. Yusof, A. Idris, E. Abdullah. PAPR reduction in FOFDM system using group codeword shifting technique. *Journal of Electrical and Electronic Systems Research* **21**:121–125, 2022. <https://doi.org/10.24191/jeesr.v21i1.016>
- [36] M. Mounir, M. B. El Mashade, S. Berra, et al. A novel hybrid preconvincing-companding technique for peak-to-average power ratio reduction in 5G and beyond. *Sensors* **21**(4):1410, 2021. <https://doi.org/10.3390/s21041410>
- [37] K. Zu, R. C. de Lamare, M. Haardt. Generalized design of low-complexity block diagonalization type precoding algorithms for multiuser MIMO systems. *IEEE Transactions on Communications* **61**(10):4232–4242, 2013. <https://doi.org/10.1109/TCOMM.2013.090513.130038>